[redacted]

POST FLIGHT EVALUATION

OF RECOVERED SRV HARDWARE

PROGRAM [redacted]

JANUARY, 1965

Prepared By

Re-Entry Systems and Technology Section

Approved By

[redacted] Manager

Space Systems Programs

GENERAL (GE) ELECTRIC
Re-Entry Systems Department
A Department of the Missile and Space Divisic
3198 Chestnut Street
Philadelphia 4, Penna.

[redacted]

FOREWARD

This evaluation was performed in support of Program [redacted] by the Re-Entry Systems and Technology Section, Re-entry Systems Department, General Electric Company, Philadelphia, Pennsylvania [redacted]. Technical direction was provided by [redacted], System Engineer, Program [redacted]. Other principal contributors were: [redacted]

The cooperation and assistance of the Space Systems Division, United States Air Force is acknowledged.

[redacted]

ABSTRACT

Recovered hardware (debris) from a Program [redacted] re-entry vehicle were furnished to the Re-Entry Systems Department for evaluation. This vehicle had flown [redacted] days in orbit before commencing a re-entry trajectory because of atmospheric drag effects. Exposure to the tropical [redacted] environment followed impact. Debris consisted of sections of the forebody and attach hardware, and pieces of the thermal cover and parachute.

The phenolic-nylon heat shield had evidence of: (1) local cracking in orbit, (2) development of a protrusion during orbit or early re-entry, and (3) curling at edges adjacent to stress relief grooves during re-entry. Missile performance capability is not limited by these conditions. Shield degradation during re-entry matched semi-empirical correlations developed from previous flight data within reasonable tolerances. Degradation rate parameters were determined from shield material exposed ot the actual re-entry environment. The performance of the current gap filler was confirmed. Parts, parachute, and thermal cover evaluations suggest that the afterbody was not directly exposed to re-entry heating while tumbling, or prior to R/V stabilization and separation. Magnesium mounting ring and ring-to-liner bond investigations indicated satisfactory performance.

Results confirm adequacy of the present design and vehicle quality.

[redacted]

TABLE OF CONTENTS

Page

LIST OF FIGURES

Page

[redacted]

LIST OF TABLES

(o)

Page

[redacted]

I. INTRODUCTION

Recovered re-entry vehicles and materials can provide information and data which cannot now be duplicated by ground tests. Ground simulations of flight environments are only limited simple approximations because of facility and technology capabilities, knowledge of flight environmental parameters, ambient natural conditions, and economy of resources. Capability for direct or remote observation during flight is also limited. Therefore the present evaluation was performed with the following objectives:

1. identification of areas where product improvements might be made
2. observation and measurement of response and performance in actual flight environments
3. increased understanding of operational capabilities
4. advancement of technology resulting from application of new data and upgrading of design techniques.

II FLIGHT PROFILE AND CONFIGURATION

The hardware received was from the R/V (apparently "A" R/V) of a [redacted] configuration spacecraft launched from The Air Force Western Test Range on a Thrust Augmented Thor Booster. Launch data, and orbital elements and data on injection were:

a. date of launch - April 27, 1964
b. Time of launch - 2325 Z (1525 PST)
c. height of apogee - 251.8 miles
d. height of perigee - 99.2 miles
e. inclination - 79.92° (geographic)
f. period - 90.87 minutes
g. eccentricity - .0211.

The spacecraft was re-oriented and stabilized after injection, and maintained stabilization and earth-orientation until the seventy-second (72nd) orbit, at which time the tumbling

mode was commenced. (The "A" R/V could not be separated according to plan at the end of this first orbital mission phase.) The spacecraft was re-stabilized on the Two hundred and forty-sixth (246th) orbit, but lost stabilization within Two days afterwards because of propellant gas depletion. Thirty days after injection, the spacecraft orbit injection configuration (see Figure 0) commenced a re-entry trajectory because of atmospheric drag effects. Impact was in Venezuela, S.A. on May 28, 1964. [redacted] a South to North trace, [redacted] Impact point coordinates were 8° north latitude, 67° west. Radar provided continuous tracking. At some point on the spacecraft descended in its trajectory, the radar noticed a change from single to

FIGURE C

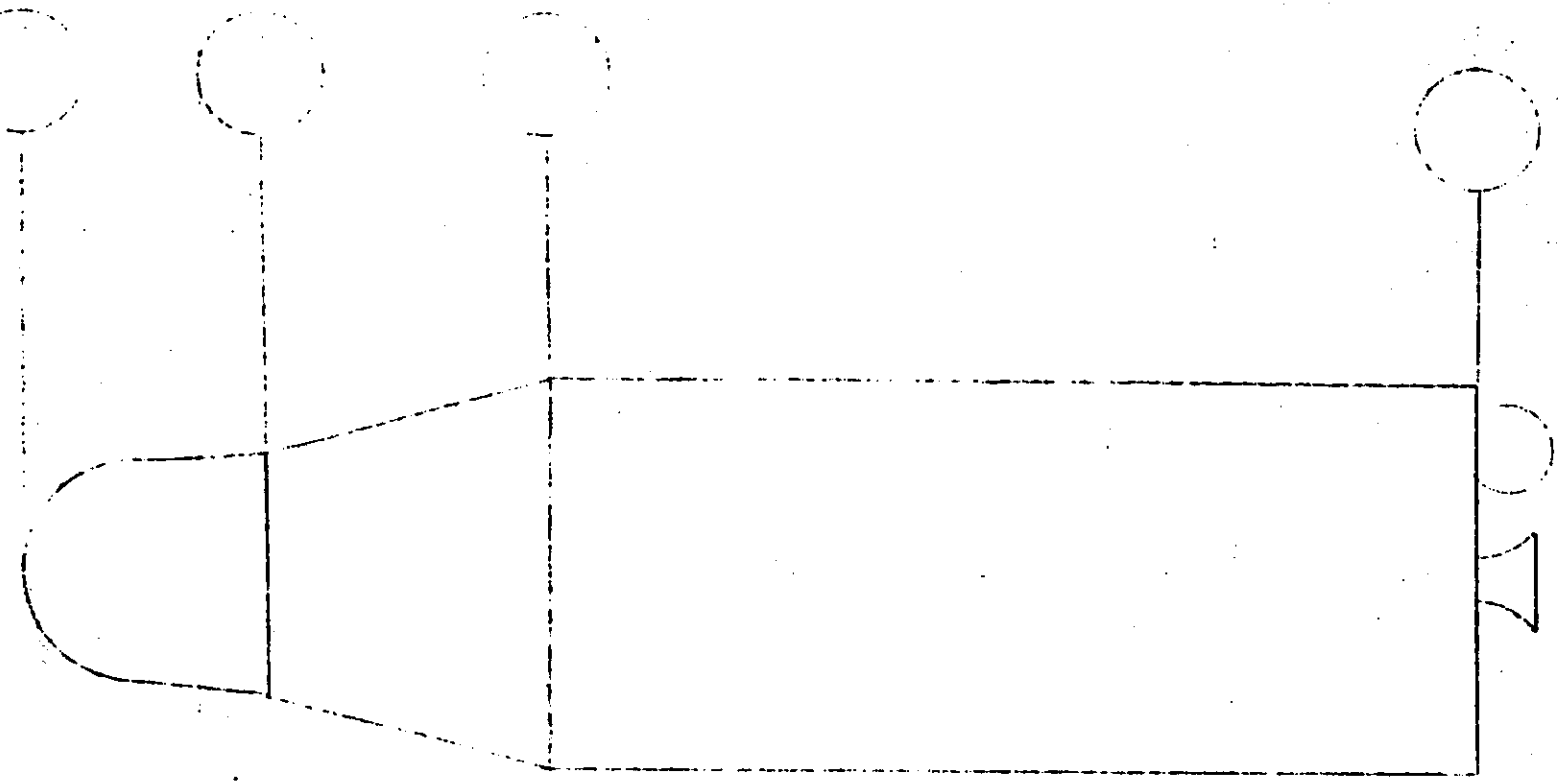

[redacted] CREW INJECTION CONFIGURATION

multiple object return. Specific location and altitude of this point, and duration of tropical exposure after impact are unknown.

III. RECOVERED DEBRIS

In composite, the pieces received constituted sections of a forebody assembly (GE drawing #198R301) with certain higher assembly items installed, and several portions of the parachute and thermal cover. Included were:

a. heat shield assembly: phenolic-nylon ablative shell and phenolic-glass structural liner, silicone rubber gap filler (GE drawing #226E590)

b. aft shield ring: phenolic-glass (GE drawing #679D122)

c. mounting ring: magnesium alloy ZE41A (GE drawing #198R306)

d. microswitch: component with aluminum bracket (GE drawing #692D911)

e. interface lug: steel part coated with solid film lubricant, molybedenum disulfide in an alkyd binder (GE drawing #10283805)

f. W1J1 interface harness connector: [redacted] part PC07H-22-55P

g. parachute: portions of fabric (GFE)

h. thermal cover: phenolic-glass (Pyropreg) (GE drawing #226E590)

i. capsule guides; phenolic-glass with steel facings (GE drawings #887C525 and #692D925)

Photographs of portions of the recovered forebody sections, Figures 1, 2, and 3, show the general condition of the heat shield and other materials received. Other portions of the shield were deeply impressed with soil. With the exception of a badly damaged and soiled section which included regions of the nose cap periphery, returned shield sections were from conical frustum of the heat shield assembly.

IV. DEBRIS EVALUATION

A. Orbit and Upper-Atmospheric Flight

Visual examination of the phenolic-nylon heat shield revealed the typical "dried mud flat" appearance of an ablative material after re-entry and cool-down. Most of the random cracks (see Figure 3) were produced after re-entry when the phenolic nylon cooled down. During re-entry when the phenolic nylon is above 500°F it deforms plastically in compression so that a sudden cooling after re-entry would produce tensile cracks. This is substantiated by the fact that most of the cracks near the free edge of the phenolic nylon are meridional in direction because of high hoop compression during re-entry with very low axial compressive stresses. Most of the cracks in the hoop direction are away from the free edges where the axial compression stresses are equal or higher than the hoop compression stresses. Several cracks were observed, however, which evidently occurred during orbital flight.

Based on the launch parameters and flight profile, β angles (angle between solar vector and orbital plane) of -50° to -35° were experienced during orbit. These conditions could result in local heat shield temperatures as low as -190°F. Minimum temperature location is shown in Figure 4. By analysis (reference 1), local shield cracking would be predicted even with no degradation of material properties (shrinkage, reduction of elongation) or compressive creep due to previous elevated temperature exposure in orbit. The cracks would occur close to the stress relief grooves, in a meridonal direction, with the most severe cracks developing at the aft-most stress relief groove. Considering the circumferential temperature distribution and the minimum temperature location for earth-oriented orbital flight, the predicted cracks would be confined to the small segment of the circumference experiencing near minimum temperatures (approximately 20 degrees of arc). Very few cracks would be expected, since those occurring would relieve the local stress levels.

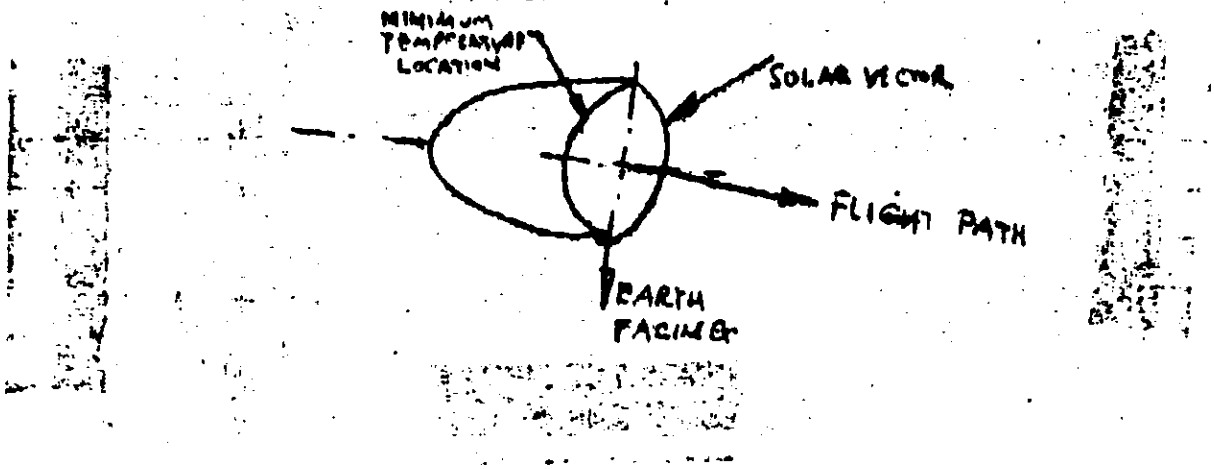

FIGURE 4

Minimum Temperature Location on Shield During Earth-Oriented Orbital Flight

The minimum temperature region for earth-oriented flight was located on the debris and the cracks examined for charring along the edges down to the phenolic glass. Only one such crack was found in this region and upon examination of the rest of the shield circumference, only two or three other similar cracks could be found, randomly spaced around the circumference. Most of the cracks still had virgin material at the base next to the phenolic glass, indicating that these cracks occured during the latter portion or subsequent to the reentry heating period.

Based on the analytical predictions and on the fact that several cracks had charring along the edges down to the phenolic glass, the conclusion is reached that these cracks occured in orbit. The random locations probably occured due to the fact that the vehicle was stabilized inorbit for only the first four and latter two days. For most of the remaining days in orbit, the vehicle was probably tumbling. If, during this latter time, the vehicle was stabilized for three to five orbits, other portions of the circumference could also have been subjected to ~~this cold~~ very low temperatures, thus producing the additional cracks. In any event, these meridional cracks, local to the stress relief grooves, produced by in-orbit cold temperatures, are not considered detrimental to the mission performance capability of the shield system.

A trajectory was calculated from known initial orbital conditions to impact. The orbital elements which were used are defined in Section II of this report. A constraint on the trajectory was impacting in thirty days, with the given history of stabilized and unstabilized flight. Using a Harris-Priester atmosphere, this condition was satisfied. For stabilized flight throughout the observed duration of orbit, only a small amount of decay would have resulted.

The motion behavior of the vehicle can only be a subject of speculation since the aerodynamic and mass characteristics are not known. However, it is most probable that the vehicle stabilized and the R/V separated from the rest of the orbital system at a high altitude. The R/V then continued into impact. Assuming a W/CDA of 55 psf the trajectory parameters are given in Figures 5 and 6. This trajectory gives rise to the thermal shield weight loss which was observed.

B. Re-Entry and Impact

1. Thermodynamic Performance

a. Shield Performance

Post recovery measurements were taken from the aft frustum pieces of the vehicle heat shield to determine the extent of shield degradation. By use of previous flight data and simplified techniques, this data was translated into an estimate of the aerodynamic heating experienced by the R/V during re-entry.

Table I presents measurements taken from the recovered aft frustum pieces. By subtracting the remaining phenolic nylon thickness from the nominal design thickness of the shield, it was possible to obtain an estimate of the depth of local shield degradation. This data and similar data from R/V 38 is plotted as a function of vehicle axial length in Figure 7. It can be seen that the average debris degradation depth is greater than that of R/V 38 by 36% and 73% at Stations 23 and 18 respectively. A fair amount of debris data scatter is shown, but it is not in excess of the 3σ variance indicated by extensive post recovery measurements obtained from R/V 38.

Figure 8 presents a correlation of R/V 39 degradation depth as a function of the time integrated re-entry heating. The mean degradation values of Station 18 and 23 (Figure 7) were used as an argument to enter Figure 8 so that estimates of the local heating rates could be obtained. For Station 18 the integrated heating is 3770 BTU/Ft^2 and at Station 23, 2350 BTU/Ft^2. The ratio of these two values is = 63% normally, a ratio of 89% would be

FIGURE 54

RE-ENTRY PATH ANGLE, VELOCITY, AND TIME VS. ALTITUDE

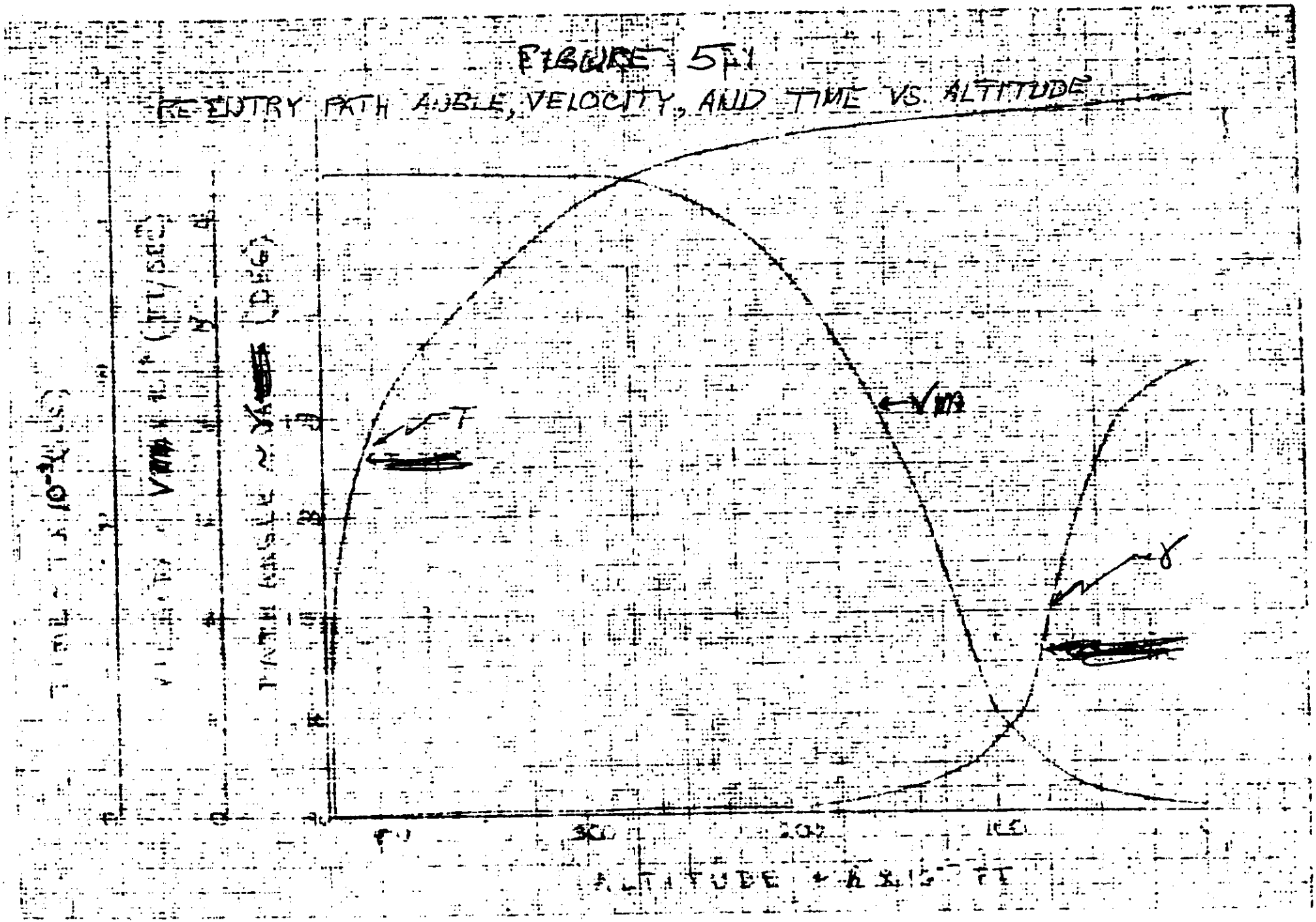

FIGURE 6.1.1

RE-ENTRY MACH NUMBER, DYNAMIC PRESSURE, AND AXIAL LOAD VS. ALTITUDE

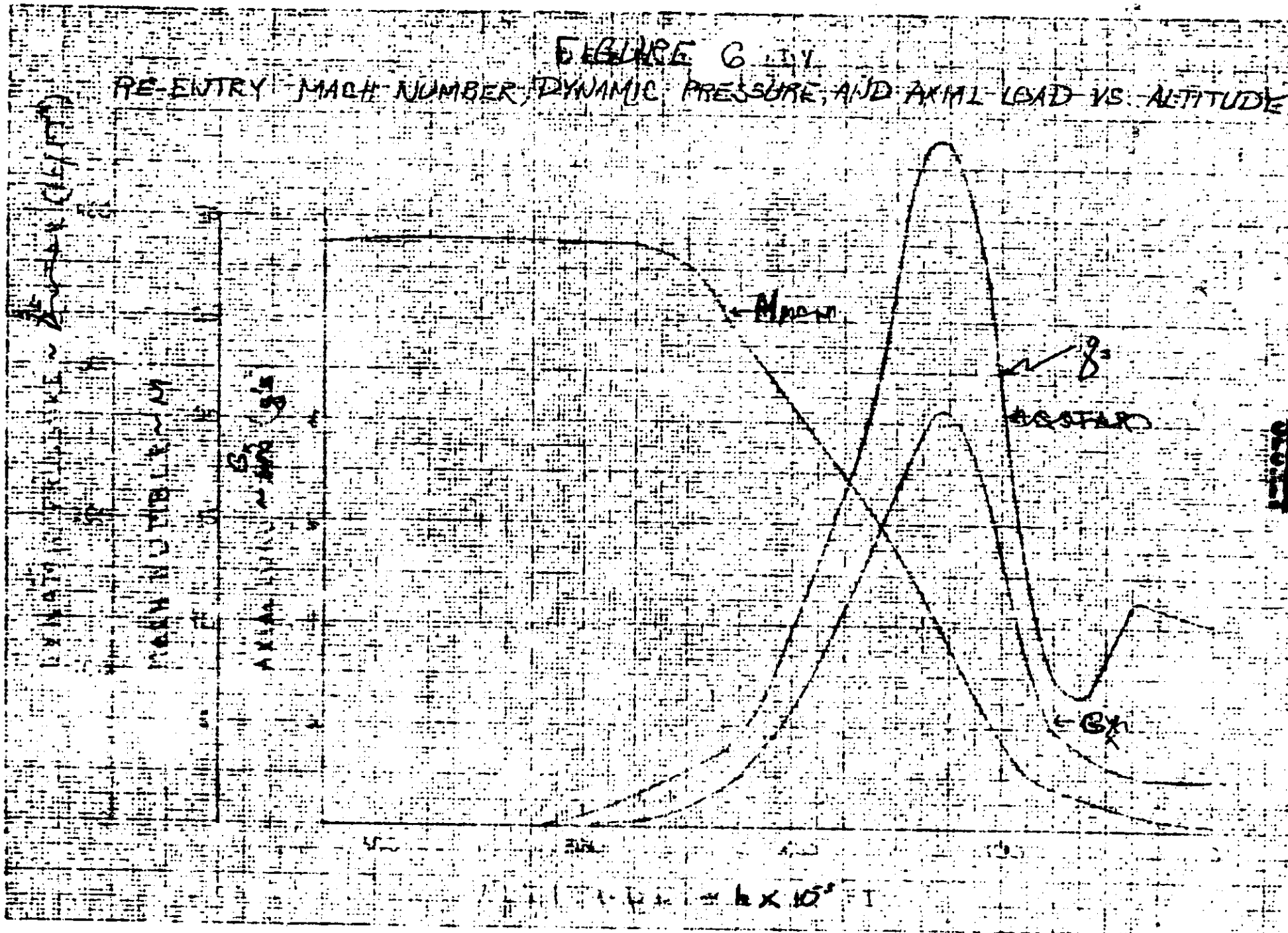

TABLE I

SHIELD DEGRADATION MEASUREMENTS

LOCATION			MATERIAL	THICKNESS IN.	
SAMPLE NO	STATION* IN.	CLOCK ANGLE DEG.	CHAR + VIRGIN PHENOLIC NYLON	VIRGIN PHENOLIC NYLON REMAINING	DEPTH OF DEGRADATION **
1	17.91	315°	0.138	0.097	0.12
1	17.91	315	0.162	0.136	0.08
2	23.4	45	0.187	0.147	0.07
3	18.4	130	0.212	0.161	0.06
4	18.4	150	0.145	0.121	0.10
5	23.4	315	0.194	0.136	0.08
6	23.4	20	0.220	0.176	0.04
6	23.4	20	0.262	0.174	0.05
7	23.4	135	0.206	0.160	0.06
8	23.4	160	0.178	0.153	0.07

AVERAGE DEPTH
OF DEGRAD.
AT STA. 23.4 = 0.06"

*Axial Distance from stagnation point.

**Based on nominal design thickness: 0.2195"

FIGURE 7

MEASURED SHIELD DEGRADATION VS AXIAL STATION

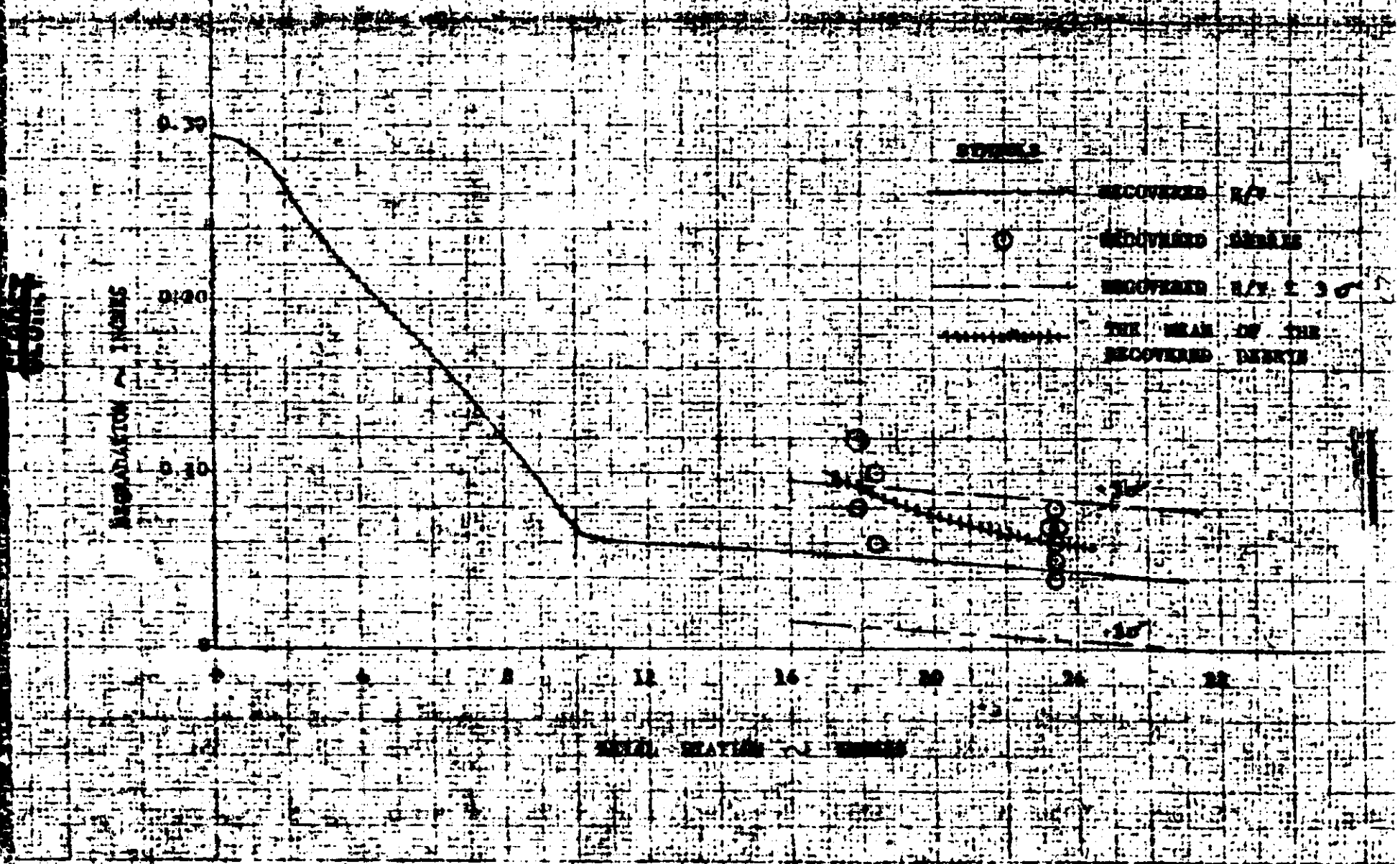

FIGURE 8

SHIELD DEGRADATION VS INTEGRATED HEAT FLUX

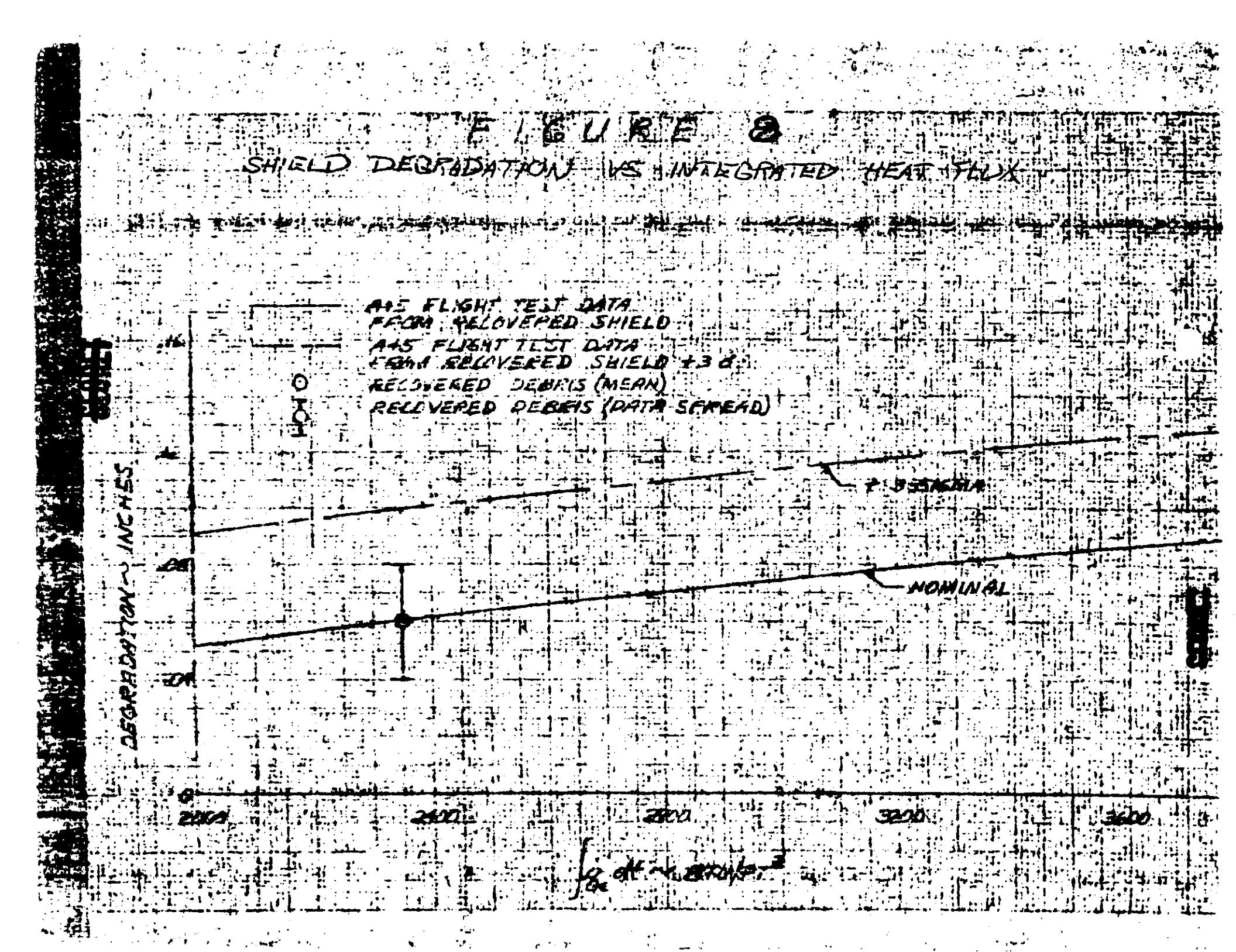

FIGURE 9

INTEGRATED HEAT FLUX VS RE-ENTRY HEATING PARAMETER

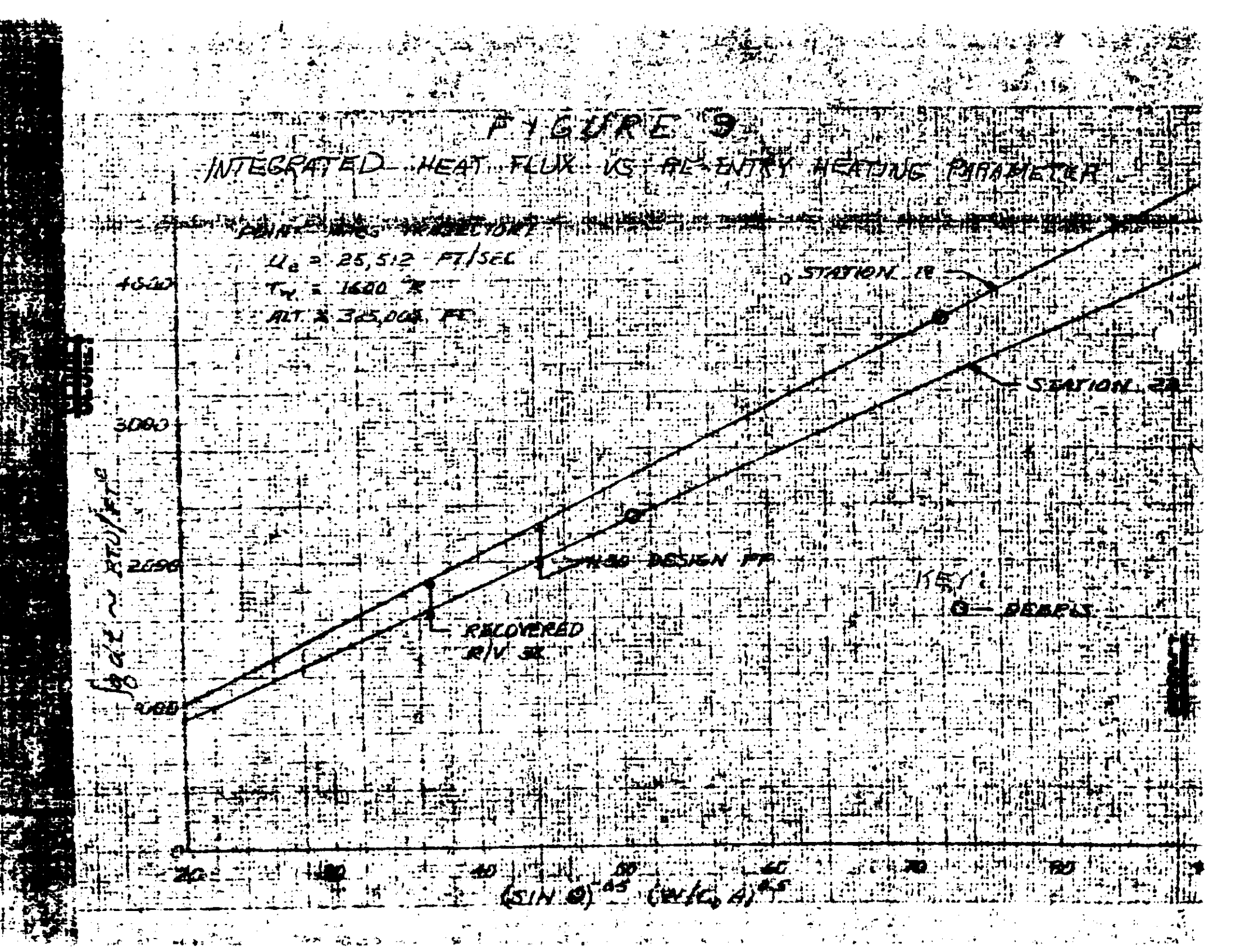

expected as $\int q\,dt)_{laminar} = \frac{1}{-\frac{1}{2}} * \rightarrow *$

In order to estimate the possible re-entry path angle extremes indicated by the shield degradation, Figure 9 was developed. This figure presents the dependency of the time integrated re-entry heating as a function of re-entry path angle and ballistic coefficient. Employing the integrated heating obtained from Figure 8 as an argument

$$(\sin\theta)^{-\frac{1}{2}} \qquad (W/C_{DA})^{\frac{1}{2}}$$

extremes of 51 and 72 were obtained for Stations 23 and 18 respectively. Assuming a constant hypersonic ballistic coefficient of 55 yields a path angle range of $1^{o}.13'$ to 36' at an altitude of 325,000 feet. This is a rough estimate of the path angle which fails to take into consideration the vehicle angle of attack and the reported delay of separation of the R/V from the system. Both of these events would cause a significant variation in the vehicle's apparent hypersonic ballistic coefficient.

b. Afterbody Performance

Several portions of the parachute and thermal cover were obtained. The lack of evidence of heating would suggest that these pieces were not exposed to attached boundary layer heating rates. Therefore, it would appear that during the early portion of the re-entry, when normally the R/V has an angle of attack greater than 90^{o} which would cause the occurrence of an attached boundary layer on the thermal cover, the spacer section was still attached to the R/V. Subsequent to the decay of the angle of attack to less than 90^{o}, this member probably was separated from the vehicle, but subsequent chute cover heating rates resulting from wake heating were not high enough to cause significant depolymerization of the Pyropreg cover. This opinion is further substantiated by the condition of the antenna stub and insulated wires exposed in the aft area. None gave an indication of experiencing appreciable heating. An organic film noted on the cover surface is attributed to decomposition products from other materials.

e. Shields

Examination of the aft shield section revealed evidence that cracks were present in the shield during the re-entry heating period. Vertical surfaces of the shield crack were slightly charred down to the phenolic glass liner. These cracks did not alter shield thermodynamic performance.

d. Stress Relief Grooves

A profile view of the saw cut at Station 21 indicated that the local bond between the shield and liner had failed. This resulted in warping or curling of the phenolic nylon shield in the following manner:

FIGURE 10

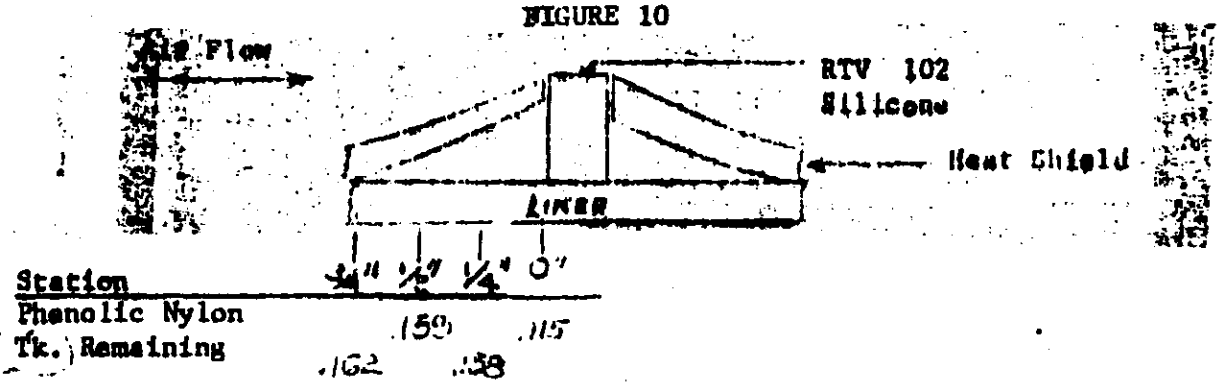

SKETCH OF SHIELD CROSS-SECTION SHOWING EDGE CURLING

As the remaining thickness of the virgin phenolic nylon decreased near the stress relief grooves, ~~as you approached the saw cut~~, it can be concluded that the curvature was present during the heating period. The increased body angle with respect to the air stream resulted in a local pressure and heating increase which lead to greater depths of shield degradation. A similar conclusion was drawn from the recovered R/V 38.

e. Ablative Gap Filler

The ablative gap filler for the recovered debris was RTV 102 silicone rubber. By comparison of its thermal degradation with that of the phenolic nylon shield it can be concluded that its performance is compatible with the shield material; hence, fully satisfactory for this application. The earlier flights had employed polysulfide PR1221 which had also demonstrated satisfactory thermodynamic performance.

Gap filler adhesion to the phenolic nylon was maintained in the recovered samples. Surface level erosion of the RTV 102 was slightly higher than that of the phenolic-nylon char remaining on the returned samples. No indications of swelling and void formation as a result of orbital thermal-vacuum or re-entry exposure were present.

2. Materials Performance

a. Degradation Kinetics

Thermogravimetric and Differential Thermal Analyses (TGA's and DTA's respectively) were performed to define shield degradation as a function of depth from the surface. Samples were taken from a coring removed from a randomly selected location on the shield skirt. Sample depths were: (1) at the char/virgin material interface, nominally the top third; (2) down 1/16" from (1), nominally the middle third; and (3) down 1/16" from (2), nominally the bottom third. Material from the trim ring of a production heat shield was used as a base reference. Examination of the DTA thermograms Figures 10 and 11, and 12 show that the top third material does not exhibit an endotherm at ~800°F, while the deeper samples do in varying degrees. The thermogram of Figure 10 represents a sampling from the char/virgin material interface. A temperature of 800°F probably corresponds to the "melting" of the phenolic resin, although the exact temperature is a function of curing cycle, etc. The peak at 475°F corresponds to the melting of nylon reinforcement. The intensity of this peak varies with the depth indicating that during re-entry the phenolic resin surface receded approximaterly 1/16 of an inch.

Thermogravimetric analysis (TGA) curves were run on samples from the same core and depths as the DTA samples. In addition, a reference sample was run to make comparison more complete. The top third curve showed a marked lower residual weight fraction at a given temperature than the deeper or reference samples did. ~~standard or the unablated portions of the specimen used~~: Figures 13, 14, 15, and 16 are thermograms of the reference ~~standard~~, and top, middle, and bottom thirds of the phenolic-nylon shield samples. Figure 17 is a cross-plot of the ratio of (residual weight fraction of the reference material)/(residual fraction of the debris) versus depth, at selected temperatures. Data was taken from the appended TGA curves. Figure 18 is a cross-plot of DTA data: ΔT (the differential temperature of deflection on the ΔT axis) versus depth, at selected temperatures for the same material samples. The same gradation is shown as is in Figure 17.

DTA THERMOGRAM OF TOP THIRD PHENOLIC NYLON SAMPLE

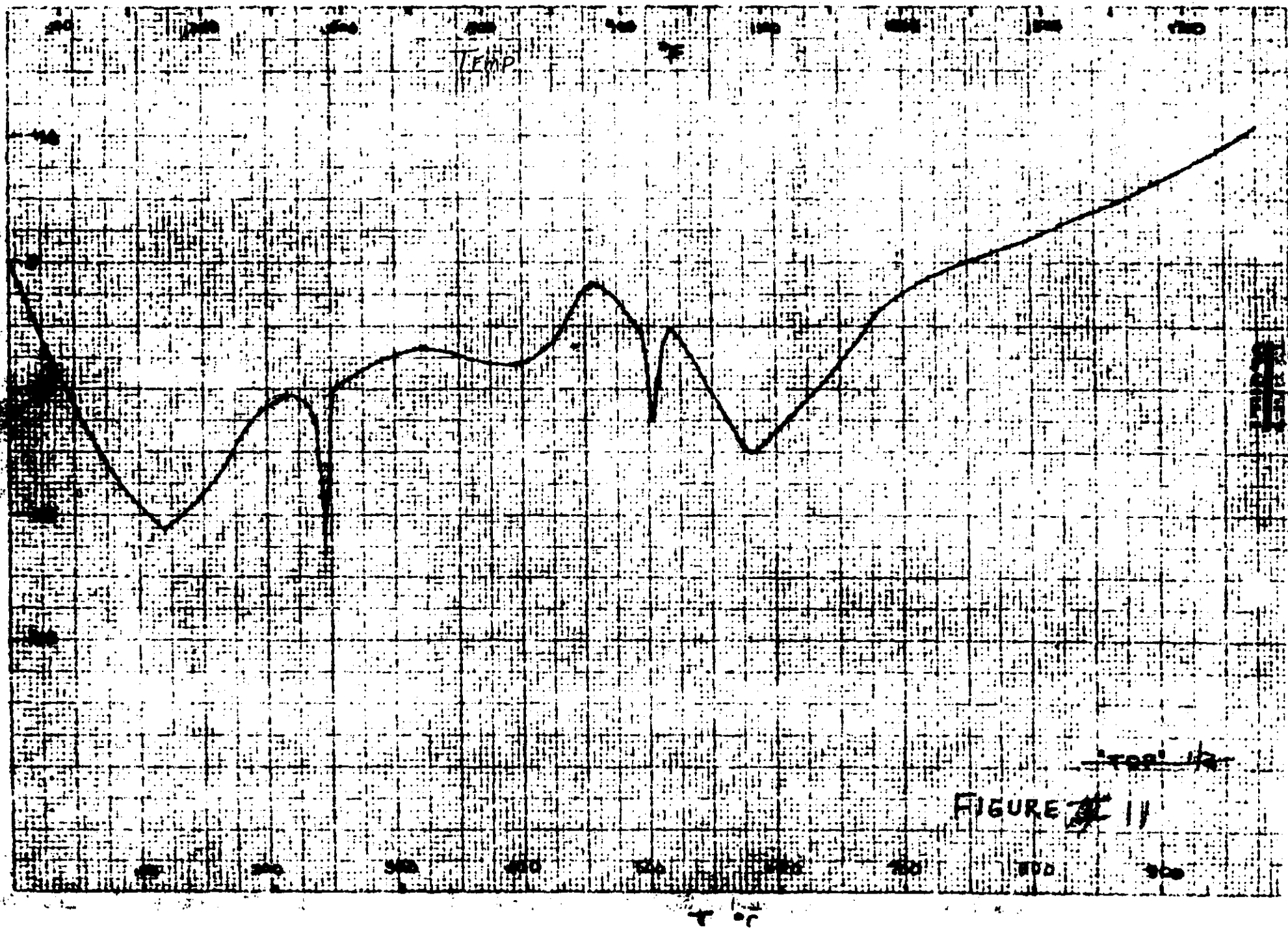

FIGURE II

DTA THERMOGRAM OF MIDDLE THIRD PHENOLIC - NYLON SAMPLE

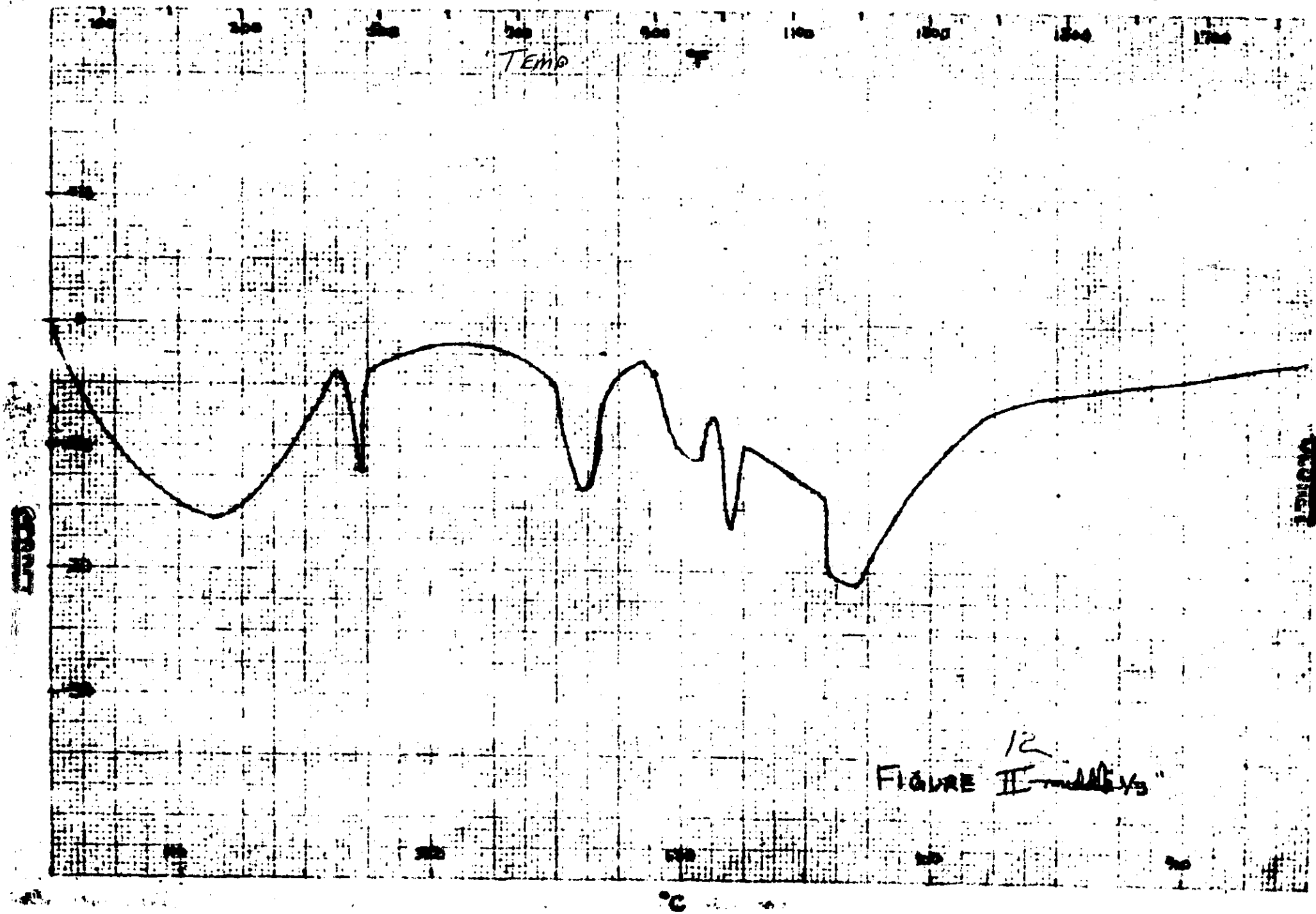

FIGURE 12

DTA THERMOGRAM OF BOTTOM THIRD P-N SAMPLE

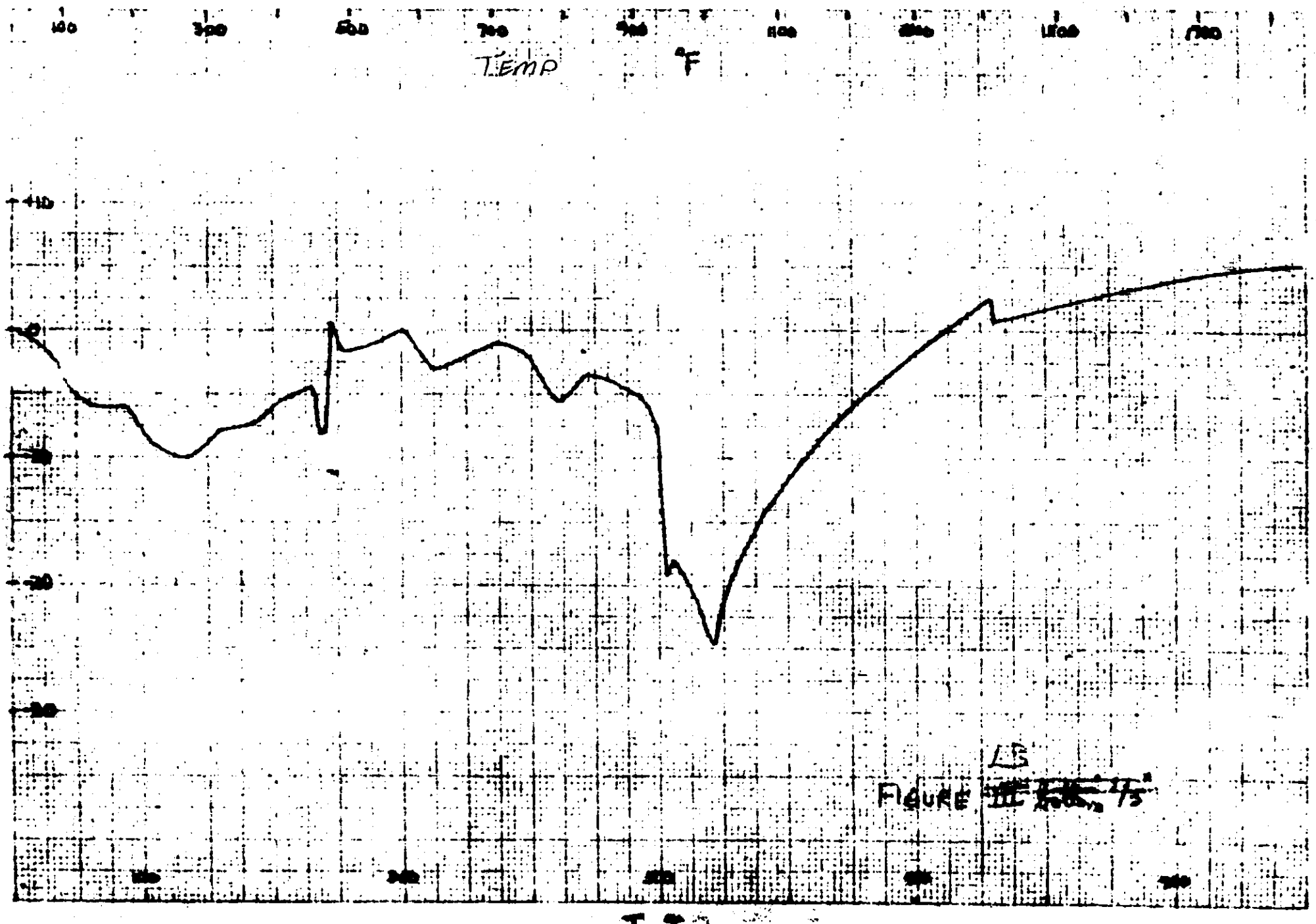

Figure 15